Journal of Power Sources 236 (2013) 145–150

Contents lists available at SciVerse ScienceDirect

Journal of Power Sources

journal homepage: www.elsevier.com/locate/jpowsour

Development of a novel and safer energy storage system using a graphite cathode and Nb_2O_5 anode

Gumjae Park [a,1], Nanda Gunawardhana [b], Chulho Lee [a], Sang-Min Lee [a], Yun-Sung Lee [c], Masaki Yoshio [b,*]

[a] Battery Research Center, Korea Electrotechnology Research Institute, 28-1 Seongju-dong, Changwon 642-120, Republic of Korea
[b] Advanced Research Center, Saga University, 1341 Yoga-machi, Saga 840-0047, Japan
[c] Faculty of Applied Chemical Engineering, Chonnam National University, 300 Yongbong-dong, Gwangju 500-757, Republic of Korea

HIGHLIGHTS

- A novel energy storage system was developed using KS-6 graphite cathode and Nb_2O_5 anode.
- Proposed charge/discharge mechanism of KS-6/Nb_2O_5 full cell using XRD and 4-electrode cell data.
- Enhanced the safety of lithium ion batteries.

ARTICLE INFO

Article history:
Received 21 August 2012
Received in revised form
16 October 2012
Accepted 25 October 2012
Available online 9 February 2013

Keywords:
Novel energy system
Graphite cathode
Niobium oxide anode
Intercalation/de-intercalation

ABSTRACT

A novel energy storage system employing a KS-6 graphite cathode and niobium (V) oxide (Nb_2O_5) anode was developed with a 1:1 weight ratio of cathode to anode. The cell, with a voltage range of 1.5–3.5 V, showed higher capacity and better cycle performance than those of cells with other voltage ranges. At 1C and 35C rates, this cell delivered 57 and 26 mAh g^{-1}, respectively. A graphite cathode can be increased to approximately 5.2 V, which is well above the LIB cathode material, without causing safety issues, and the operating voltage of the Nb_2O_5 anode was greater than that of the lithium deposition voltage. *In situ* X-ray diffraction results at various states of charge indicated that the mechanism of this energy storage system was intercalation and de-intercalation of PF_6^- and Li^+ in the KS-6 graphite cathode and in the Nb_2O_5 anode. This novel energy storage system was inherently safe because 1) no oxygen is released from cathode materials, 2) no lithium dendrite is used at the anode, and 3) there was no possibility of overcharge from the electrode/electrolyte reaction.

1. Introduction

Recyclable energy storage systems have been of interest because of increasing fuel costs and environmental aspects. Among them, rechargeable lithium ion batteries (LIBs) and electric double layer capacitors (EDLCs) are the most likely candidates for alternative energy storage systems [1–3]. LIBs are a promising portable power source device due to higher volumetric and gravimetric energy densities compared with those of other rechargeable battery systems [4]. However, LIBs have an insufficient power density and safety problem, so it is difficult to apply them to high powered devices. Several LIB fires have been reported due to deposition of lithium and/or other metal ions on the graphite anode, which can lead to a short circuit between the anode and cathode [5]. Additionally, electrolyte can react with cathode material in a charged stage resulting in decomposition of the cathode material and leading to release of oxygen from the cathode structure, which could trigger a dangerous explosion [6,7]. Unlike LIB, EDLCs have a high power density and longer cycle life compared with those of LIBs, because the storage of charge on the electrode is in an adsorption reaction at the interphase of both electrodes [8,9]. However, EDLCs have smaller energy density due to low capacity and average working voltage [10,11]. Many researchers have made efforts to improve the energy density of EDLCs. One of these is the hybrid supercapacitor of an asymmetrical system in which the electrode of a secondary lithium battery replaces one of the activated carbon electrodes [12,13]. This results in a significant increase in overall energy density due to the decrease in working voltage and an increase in negative electrode capacity. A megalo capacitance capacitor, developed by Yoshio et al., is a candidate for improving the energy density of a EDLC [14–16]. This capacitor

* Corresponding author. Tel./fax: +81 952 20 4729.
E-mail addresses: gjpark@keri.re.kr (G. Park), yoshio@cc.saga-u.ac.jp (M. Yoshio).
[1] Tel.: +82 55 280 1665; fax: +82 55 280 1590.

0378-7753/$ – see front matter © 2013 Elsevier B.V. All rights reserved.
http://dx.doi.org/10.1016/j.jpowsour.2012.10.102

replaces active carbon with graphitic carbon as the cathode material. The charge storage mechanism for the positive graphite material is principally concerned with specific anion adsorption and the intercalation of anions into the graphite positive electrode, which can be suppressed using a specific graphite electrode. This capacitor also has high energy density compared with that of a conventional EDLC because of high operating voltage and capacity. We have also found that graphite can accept large-sized anions in a non-aqueous solution.

By combining two asymmetric capacitors, we have recently developed an electrochemical power source using a graphite cathode and metal oxides, in particular, MoO_3 and TiO_2 anodes [17–19]. However, these systems did not show good cycleability which might be caused by MoO_3 and TiO_2 anodes during our preliminary studies. When MoO_3 and TiO_2 used as anode in these systems, the cathode was charged to >5.25 V during most of the test. At such high voltage, deep intercalation of PF_6^- anions into the graphite layer occurs, which deteriorates the pristine graphite structure. To reduce the working voltage of graphite and the amount of PF_6^- intercalation into graphite layers at end of charged state, we have investigated other possible metal oxides to replace MoO_3 and TiO_2. Among other metal oxide materials, Nb_2O_5 [20–22] is a possible anode material application for secondary lithium batteries. Nb_2O_5 has several structures such as hexagonal (TT-type), orthorhombic (T-type), and monoclinic (H-type) due to the synthesis conditions. Among these Nb_2O_5 materials, orthorhombic Nb_2O_5 has reversible capacity due to the reversible structure change during the charge–discharge process, although it has lower capacity than that of monoclinic Nb_2O_5.

In this study, we propose a safer novel energy storage system, consisting of a graphite cathode and Nb_2O_5 anode with anion and cation intercalation, respectively. We also investigated the electrochemical behavior of this novel energy storage system using a galvanostatic charge–discharge test. *In situ* X-ray diffraction (XRD) measurements were carried out at various stages of charge for both electrodes to understand the mechanism of energy storage in this system during the charge process. The operating voltage of the cathode and anode during cycling was obtained with a four-electrode cell, and we examined the potential of Li/Nb_2O_5 and Li/KS-6 half-cells.

2. Experimental

Artificial graphite KS-6 (Timcal. Co. Ltd., Bodio, Switzerland) was selected as the cathode material, whereas common commercial Nb_2O_5 (Wako Co. Ltd., Osaka, Japan) was used as the anode material for the new energy storage system. Powder XRD (MINIFlex II, Rigaku, The Woodlands, TX, USA) using CuKα radiation was employed to identify the intercalation of the anion and the structural changes in the positive and negative electrodes during cycling. *In situ* XRD was conducted with a homemade cell, as described previously [16]. The device was assembled in an argon-filled glove box to prevent any reaction with moisture in the air. It consisted of two electrodes separated by glass fiber filters soaked with electrolyte. The electrodes for *in situ* XRD were prepared by mixing 80 wt% active material, acetylene black, and poly(vinylidene-fluoride-co-hexafluoropropylene) binder dissolved in a *N*-methyl-2-pyrrolidone solution. The KS-6 graphite cathode and Nb_2O_5 anode materials were fabricated with 10 mg of accurately weighed active material and 6 mg of conductive binder (4 mg of Teflonized acetylene black and 2 mg of acetylene black) to investigate electrochemical properties using a CR2032 coin-type cell. They were pressed on 200 mm^2 stainless steel mesh, which was used as the current collector under a pressure of 300 kg cm^{-2}, and dried at 160 °C for 4 h in a vacuum oven. The half cells were made of a lithium metal anode (Cyprus Foote Mineral Co., Silverpeak, NV, USA) separated by two glass fibers. The electrolyte was a mixture of 1 M $LiPF_6$-ethylene carbonate (EC)/dimethyl carbonate (DMC) (1:2 by vol., Ube Chemicals, Yamaguchi Japan). The charge and discharge current density was 100 mA g^{-1} with a cut-off voltage of 3.0–5.4 V for the KS-6 graphite cathode and 1.0–3.0 V for the Nb_2O_5 anode at room temperature, respectively.

The cathode and anode of the novel energy storage system were fabricated with 10 mg of accurately weighed active material and 6 mg of conductive binder. The test cell, in which the weight ratio of the cathode to anode was 1:1, was made of the cathode and anode separated by glass fiber. The charge and discharge current density was 100 mA g^{-1} with various cut-off voltages (0–3.5, 1.5–3.3, 2.0–3.5 V, 1.5–3.5, and 2.0–3.5 V) at room temperature (25 °C).

Four-electrode cells were also constructed to trace the positive and negative electrode potentials during independent cycling. The graphite cathode electrode, Nb_2O_5 anode electrodes, and the two reference electrodes as Li metal were dipped into the electrolyte contained in the glass cell. During the process of galvanostatic charge–discharge between the cathode and anode electrodes, the potentials of both with respect to the reference electrode were measured with an auxiliary potentiometer. The electrode potentials in the electrolyte are generally reported against the Li metal. The total voltage of the energy storage system actually equaled the difference between the cathode and anode electrode potentials.

3. Results and discussion

Fig. 1 shows the XRD results of the (a) KS-6 graphite and the (b) Nb_2O_5 powders. We used Si powder as a standard material to correct for the graphite (002) peak. KS-6 graphite exhibited a (002) peak at $2\theta = 26.46°$, which agreed well with the interlayer distance

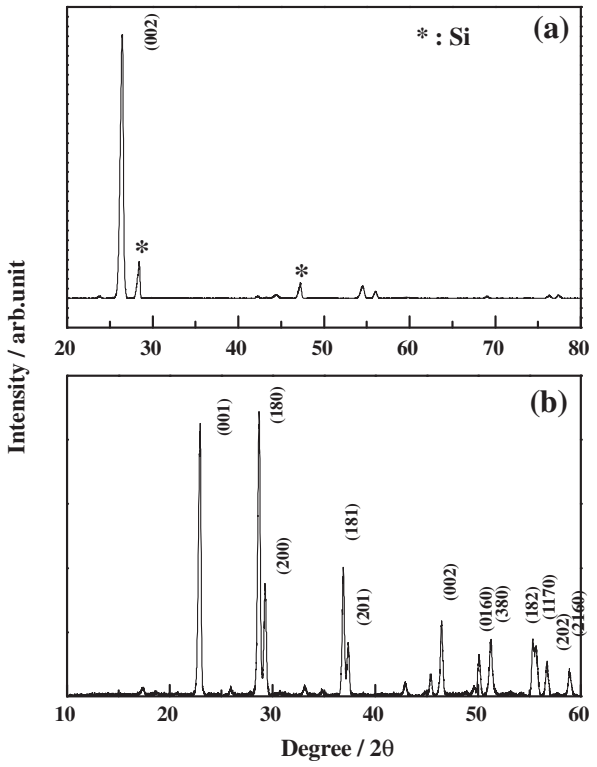

Fig. 1. The X-ray diffraction (XRD) results for the (a) KS-6 graphite cathode and (b) Nb_2O_5 anode.

value, $d_{(002)}$, of 3.36 Å. The KS-6 graphite belongs to graphite by Franklin's definition, because the $d_{(002)}$ value is < 3.440 Å [23], but the (002) peak intensity is not as high as natural graphite. The XRD patterns of the KS-6 graphite were in the range of $2\theta = 40–50°$. The KS-6 graphite had lower peak intensities of rhombohedral (101) and (102) lines than those of the hexagonal (100) and (101) lines. The XRD results showed that the KS-6 graphite had 24% rhombohedral phase content in the graphite. The KS-6 had about a 6 μm average particle size and 18 $m^2\ g^{-1}$ of specific surface area. The electrochemical properties of KS-6 as the anode material in secondary lithium batteries have been studied previously [24,25].

The Nb_2O_5 used in this study had an orthorhombic structure with lattice parameters of $a = 6.05$ Å, $b = 29.04$ Å, and $c = 3.86$ Å, which was indexed to JCPDS card #27-1003 of Nb_2O_5.

Fig. 2 shows the charge/discharge curves of the (a) Li/1 M $LiPF_6$-EC/DMC (1:2)/KS-6 graphite half cells. The test conditions were a current density of 100 mA g^{-1} with a cut-off voltage from 5.3 to 3.0 V. The anion acceptor type of graphite intercalated compound has been reported by many research groups, but its electrochemical properties are unclear, because the electrolyte oxidizes with the cathode material at the higher voltage region. The charge–discharge curves of KS-6 graphite showed a bent-line voltage profile. When the voltage was limited to 5.3 V, it did well work at the voltage regions. During the charging process, voltage increased rapidly up to 4.65 V and then slowed down. Thus, capacity started to increase at this point. The graphite electrode had increasing voltage plateaus and showed voltage regions of 4.65–4.8 V, 4.85–5.1 V, and 5.1–5.25 V due to a stage change according to intercalation of the PF_6^- anion into graphite. The voltage plateaus for the second cycle showed higher voltage than that of the first cycle due to electrolyte decomposition and formation of an SEI film during the first charge process. During the discharge process, KS-6 graphite showed an initial decrease until 4.9 V and then gradually decreased to 3.8 V. The initial discharge capacity of KS-6 graphite was 86.5 mAh g^{-1}.

Fig. 3 shows the charge/discharge curves of the (a) Li/1 M $LiPF_6$-EC/DMC (1:2)/Nb_2O_5 half cell. The test conditions were a current density of 100 mA g^{-1} with a cut-off voltage from 3.0 to 1.0 V. The Li/Nb_2O_5 half cell showed linear voltage, in which the voltage decreased rapidly to 2.0 V and then decreased slowly from 1.9 to 1.0 V. It exhibited a long voltage plateau between 1.9 and 1.0 V and 186 mAh g^{-1} of initial discharge capacity for Li/Nb_2O_5. The second discharge capacity decreased about 20 mAh g^{-1} compared with that of the first discharge capacity due to electrolyte decomposition during the first discharge process. The charge curve also exhibited a long voltage plateau between 2.1 and 1.0 V and 165 mAh g^{-1} of charge capacity. The retention rate of Li/$LiPF_6$-EC/DMC (1:2)/Nb_2O_5 cell was 90% during 2–50 cycles. It showed a low voltage plateau between 2.0 and 1.0 V to Li metal for the charge/discharge process in the Li/Nb_2O_5 cell, so we would expect to obtain high energy density because of the decreasing working voltage of the anode material compared with that of activated carbon. When we applied anode material to graphite/metal oxide energy storage systems, the voltage of graphite cathode was lower than that of KS-6/MoO_3 and KS-6/TiO_2 systems. It also improved safety due to no lithium deposition on Nb_2O_5 because of the high intercalation voltage (1.5 V. Li/Li^+) compared to that of a LIB using a graphite anode.

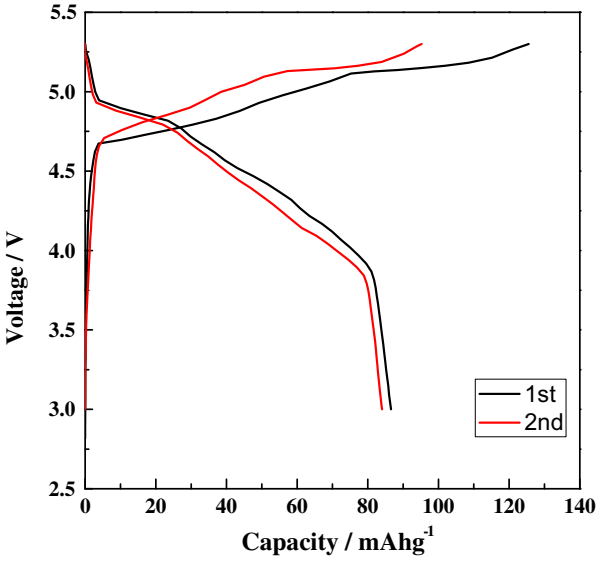

Fig. 2. Typical charge–discharge curves for Li/1 M $LiPF_6$-EC/DMC (1:2)/KS-6 graphite with a current density of 100 mA g^{-1} between 5.3 and 3.0 V at room temperature.

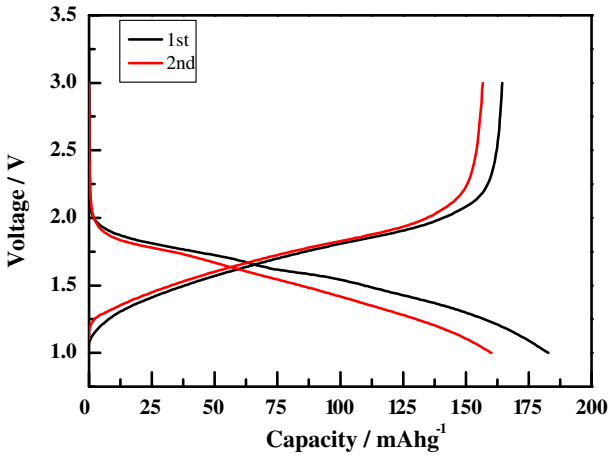

Fig. 3. Typical charge–discharge curves for Li/1 M $LiPF_6$-EC/DMC (1:2)/Nb_2O_5 with a current density of 100 mA g^{-1} between 3.0 and 1.0 V at room temperature.

Fig. 4 shows (a) the initial charge–discharge curves and (b) cycle performances obtained at different voltage regions for the KS-6/Nb_2O_5 novel energy storage system with a weight ratio of 1:1. The charge/discharge curves of the cells revealed a bent line containing two linear portions. First, the cell voltage rose sharply to 2.7 V, but energy storage in the cell at this step was rather small, which means the amount of anion adsorption at the graphite edged plane was small. The climb-up speed voltage was slowed down; thus, capacity increased rapidly from 2.7 to 3.5 V. This result indicates that the mechanism of this energy storage system was intercalations between layers of graphite at the second linear portion. This energy storage system obtained about 3.1 V of average voltage, which is higher than the average voltage of a megalo-capacitance capacitor that exhibits about 2.75 V of average voltage. The discharge curve decreased slowly up to 2.0 V and then decreased quickly up to the limit voltage. The initial discharge capacities of the cells at 3.5–0 V, 3.5–1.5 V, 35–2.0 V, 3.3–1.5 V, and 3.3–2.0 V were 55, 48, 45, 33, and 29 mAh g^{-1}, respectively. As maximum cell voltage increased from 3.3 to 3.5 V, cell capacity increased from 33 to 45 mAh g^{-1} at 1.5 V of minimum voltage. These cells have an advantage in terms of energy density at a maximum voltage of 3.5 V because of their high average working voltage and high capacity compared to cells with tested maximum voltage of 3.3 V during discharge. The cell had higher initial discharge capacity of 55 mAh g^{-1} between 3.5 and 0 V and exhibited good cycle performance until the cycle 20; however, capacity decreased abruptly to 30 mAh g^{-1} at cycle 50 with a cycle retention rate of 54%. This

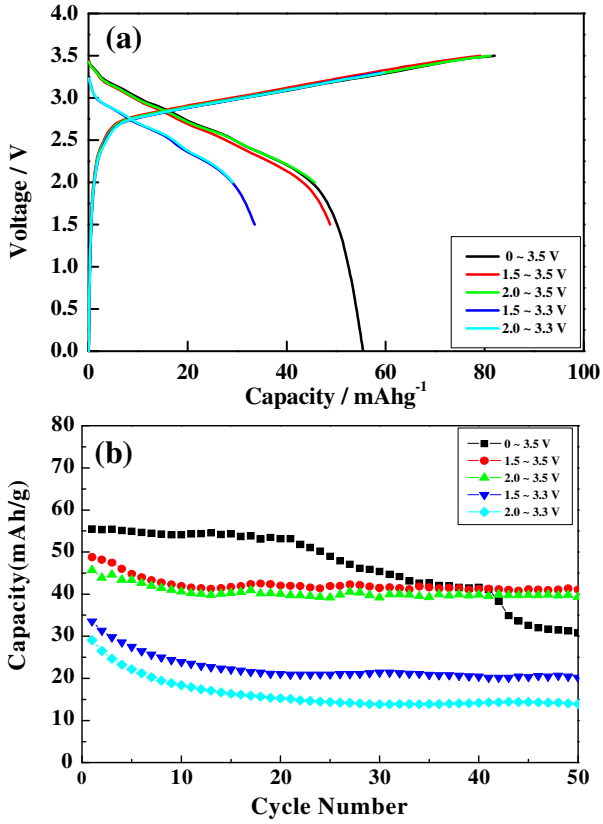

Fig. 4. (a) Initial charge–discharge curves (b) cycle performance for the KS-6/Nb_2O_5 cells with a weight ratio of 1:1 for various cut-off voltage ranges (3.5–0 V, 3.5–1.5 V, 3.5–2.0 V, 3.3–1.5 V and 3.3–2.0 V) with current density of 100 mA g^{-1}.

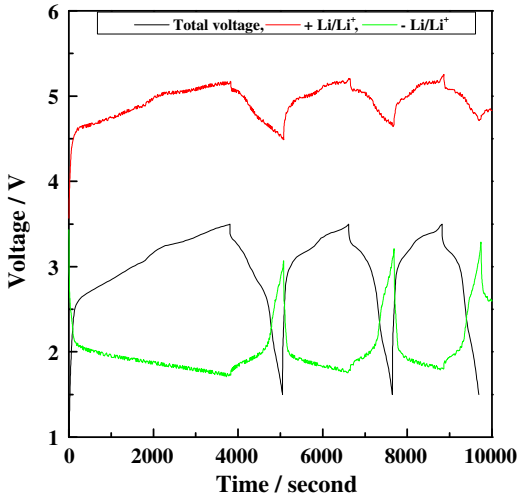

Fig. 5. Potential profiles of the KS-6/Nb_2O_5 cell during the galvanostatic charge–discharge process. The cathode and anode electrode had the same weight of active material.

seemed to be due to degradation of the graphite from PF_6^- intercalation and repetition from intercalation to deintercalation in the graphite layer. The cell at voltages from 3.5 to 1.5 and 2.0 V showed better cycle performance than that of a cell between 3.5 and 0 V. The cycle retention rates at voltages from 3.5 to 1.5 and 2.0 V were 85 and 86%, respectively. Discharge capacity dropped only in the initial 10 cycles, and discharge capacity was retained after cycle 10. Retention rate improved by increasing minimum voltage from 0 to 1.5 V. A considerable number of anions may intercalate/deintercalate into the interlayers of the graphite during charge/discharge, so that the graphite electrode suffered from large volume changes that have a destructive effect on graphite, which is not good for cycleability of an energy storage system [26,27]. It is likely that PF_6^- anions remained in the graphite interlayer after discharge up to 1.5 V, so that expansion of the *c*-axis for graphite was not great compared with that of a cell discharged at 0 V, which occurs fully due to insertion and desertion from the graphite interlayer. In particular, the cell region showed the best performance in the 3.5 and 1.5 V voltage region, considering capacity and cycle retention rate.

We prepared a four electrode cell and recorded with two lithium metal references to trace the voltages of cathode and anode electrode in the KS-6/Nb_2O_5 cell during the galvanostatic charge/discharge process. Fig. 5 shows the potential profiles of the KS-6/Nb_2O_5 cell with a 1:1 weight ratio of cathode to anode during galvanostatic charge/discharge: Such a cell allows for measuring the contribution of each half-cell reaction to the overall potential profile. During the initial charge process, the ceiling voltage of graphite increased at 5.16 V, and the bottom voltage of Nb_2O_5 decreased at 1.66 V. The voltage of graphite in the system increased to 4.65 V at the first charge against the lithium reference and then slowly increased until reaching the ceiling voltage due to intercalation of PF_6^- anions in the graphite layers. Although it was not high enough to induce electrolyte decomposition of KS-6, it was not that drastic such as activated carbon, because the specific surface area of KS-6 is rather small. In contrast, the potential of the Nb_2O_5 anode electrode initially dropped to 2.1 V against the lithium metal reference. Then, it gradually decreased to the bottom voltage against the lithium reference.

In situ XRD experiments were conducted to investigate the reaction mechanisms and structural changes at the cathode and anode. Fig. 6 shows the *in situ* XRD diffractions of KS6 in the KS6/Nb_2O_5 energy storage cell at various voltages. The (002) peak appeared at 26.5° corresponding to a $d_{(002)}$ value of 3.35 Å, indicating a well-ordered graphite structure. The (002) peak started to shift lower at 2.9 V, and then the peak separated into two peaks of 24.3 and 25.3° at 3.5 V. When cell voltage reached 3.5 V, the *in situ* XRD (002) peak disappeared. Disappearance of the KS6 (002) peak during the charging process indicates that the PF_6^- anions started to insert and accumulate between interlayer spaces of the KS6 electrode. The XRD patterns suggested the stage that refers to the periodic arrangement of intercalated layers in the *c*-axis direction for intercalation of PF_6^- into the graphite electrode. Calculating gallery height and assigning a stage number for a graphite intercalation compound (GIC) require care because it is possible to co-insert solvent into the electrolyte [27–29]. Dahn's group [29] has studied the intercalation of PF_6^- anions into graphite in an Li^+-based electrolyte. They calculated the stage for intercalation of PF_6^- into the graphite interlayer using a small PF_6^- intercalated gallery height of 4.5 Å without co-inserting solvent. In our study, we identified two peaks at 24.3 and 25.3° at charges up to 3.5 V in the *in situ* XRD diffraction patterns. Based on the Bragg equation, we calculated the *d* values as 3.73 and 3.58 Å, which indicated stages of 3 and 5, respectively. The GIC stage charged at 3.5 V reached stages 3 and 5 and showed 37.3% expansion for the *c*-axis in the GIC.

Fig. 6b shows the *in situ* XRD patterns for Nb_2O_5 in the KS-6/Nb_2O_5 energy storage system. During charging, it maintained the original peak with no peak change, because capacity of the Nb_2O_5 anode was small compared to that of the KS-6 cathode during charging in the novel energy storage system.

Based on the *in situ* XRD results, we suggest a mechanism for our novel energy storage system. During charging, the mechanism at

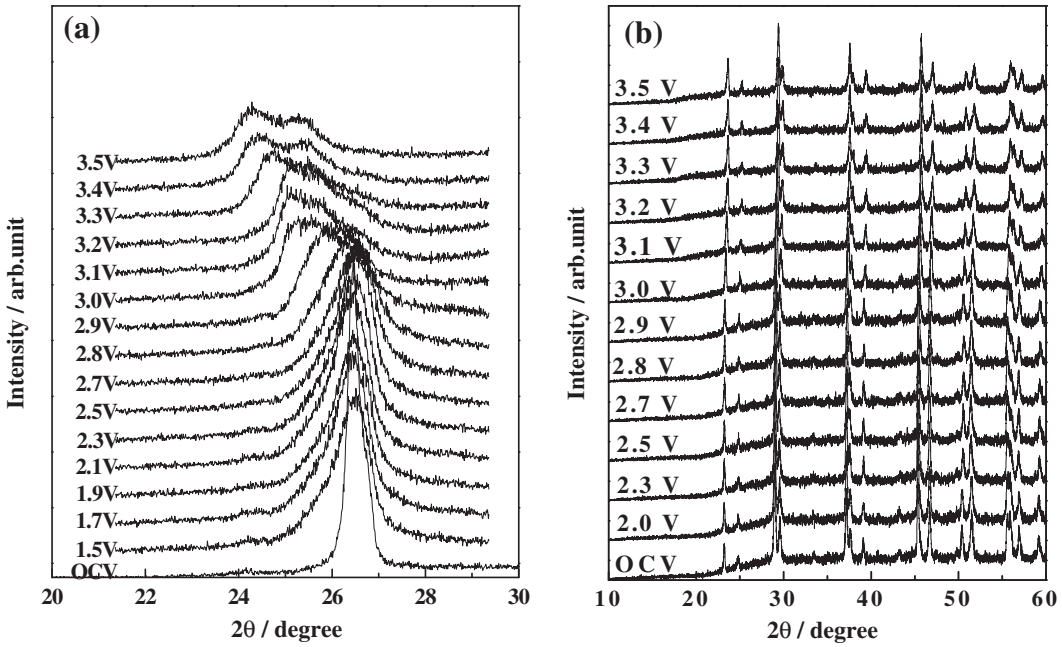

Fig. 6. *In situ* X-ray diffraction (XRD) patterns for the (a) KS-6 graphite and (b) Nb_2O_5 electrode during the initial charge process of the KS-6/Nb_2O_5 cell with a weight ratio of 1:1 for KS-6 graphite to Nb_2O_5.

the voltage region from 0 to 2.8 V is an adsorption process of PF_6^- anions in edge-plans of the graphite surface, whereas the mechanism at >2.9 V is PF_6^- anion intercalation into the graphite electrode when the weight ratio of the cathode to anode equals 1.

Fig. 7 shows the rate capabilities of the KS-6/Nb_2O_5 cell with a weight ratio of 1:1 and a cut-off voltage of 1.5–3.5 V. At a rate of 1C, the discharge capacity was 57 mAh g^{-1}. As rate in the cell increased, specific capacities decreased gradually. At a rate of 35C, the cell's discharge capacity was 26 mAh g^{-1}.

Fig. 8 is a schematic diagram of the novel KS-6/Nb_2O_5 energy storage system. When charged, the $LiPF_6$ in electrolyte was separated from Li^+ cations and PF_6^- anions, and then the PF_6^- anions intercalated in the interlayer of the graphite cathode electrode. At the same time, the Li^+ cations intercalated into the structure of the Nb_2O_5 anode electrode. Conversely, the lithium cations and PF_6^- anions were extracted from their structures during discharge and recovered in the original $LiPF_6$ in solvent. This did not reveal the category of an EDLC capacitor or battery. We think that the process in this cell is novel. This system has safety and high energy density advantages compared with those of an LIB and EDLC, respectively. In this system, the safety of energy storage can increasingly improve based on three aspects. First, the LIB cathode material usually used is a lithium transition metal oxide, which undergoes oxidation to a higher valence state during charging. In the higher voltage of a charged stage, the electrolyte reaction is induced resulting in decomposition of the cathode material, which leads to release of oxygen from the cathode structure. As there are no transition metal oxides in the positive material, there is no possibility for oxygen to be released from the cathode in the over-charged state. Second, the Nb_2O_5 operating voltage is >1.0 V vs. Li/Li^+, which is well above lithium plating and decomposition of electrolyte, so the risk of lithium dendrite formation is negligible. Finally, the $LiPF_6$ salt in the electrolyte is gradually consumed with an increase in charge state. This means that this energy storage system has high internal resistance in its over-charged state, which will suppress dangerous high current flow in extreme situations, such as a short circuit or mechanical disintegration.

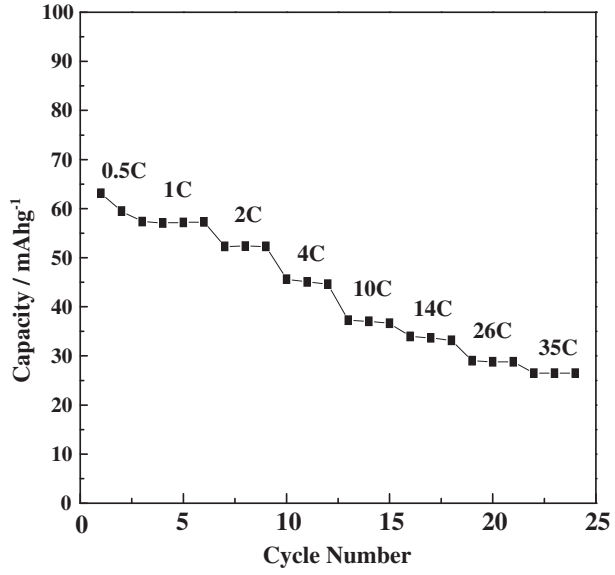

Fig. 7. Rate performance of the KS-6/Nb_2O_5 cell in the voltage range of 1.5–3.5 V.

This energy storage system will also improve two systems. One is a type of megalo-capacitance capacitor. In a previous study [30], the weight ratio was important for a megalo-capacitance capacitor in terms of high capacity and cycleability. The mechanism of a megalo capacitance capacitor is adsorption and desorption of the edged plane of the KS6 cathode material surface when the weight ratio of cathode to anode is 1. We think that controlling the weight ratio of the cathode to anode in the KS6/Nb_2O_5 energy storage system will improve capacity and cycleability. The other is a type of novel energy storage system. The graphite in an LIB has different electrochemical properties according to their structure and crystallinity [31,32]. The turbostatic disorder in the graphite probably helps depress the intercalation of anions into the graphite

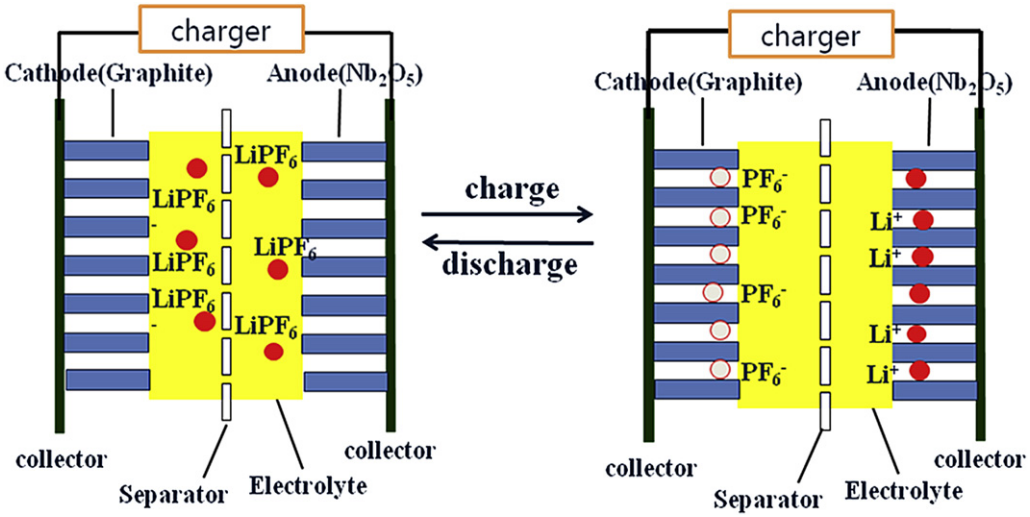

Fig. 8. Schematic diagram of the KS-6/Nb_2O_5 novel energy storage system.

interlayer. We expect that graphite with high crystallinity and low turbostatic disorder may more deeply affect anion intercalation into the graphite interlayer and show good electrochemical properties.

We are conducting detailed studies, such as electrochemical and high rate performance experiments as well as experiments on the effect of change anode/cathode weight ratio and the type of graphite.

4. Conclusion

A novel energy storage system was developed using KS-6 graphite as the cathode and Nb_2O_5 as the anode with a 1:1 weight ratio of cathode to anode. The system had high capacity and good cycleability with a cut-off voltage range of 1.5–3.5 V, and it exhibited a sloping voltage profile from 2.7 to 3.5 V during the charge process. The data obtained by *in situ* XRD revealed that PF_6^- anions intercalated into the graphite layers, which lead to some structural changes in the pristine graphite structure, whereas Li^+ ions intercalated into the Nb_2O_5 structure without structural changes during charging. The mechanism of the graphite electrode was adsorption of the graphite edged plane between 0 and 2.7 V, whereas it was anion intercalation into the graphite between 2.9 and 3.5 V. Such energy storage systems are inherently safe, because the graphite cathode raises the voltage well above the LIB cathode material without safety problems, and the operating voltage of the Nb_2O_5 anode is above the lithium deposition voltage. Moreover, overcharge is not possible, because the $LiPF_6$ salt in the electrolyte is being gradually consumed during charging.

Acknowledgment

This study was supported by a National Research Foundation of Korea Grant funded by the Korean Government (MEST) (NRF-2011-C1AAA001-0030538)

References

[1] W. Fergus, J. Power Sources 195 (2010) 939.
[2] B. Peng, J. Chen, Coord. Chem. Rev. 253 (2009) 822.
[3] A. Lewandowski, M. Galinski, J. Power Sources 173 (2007) 822.
[4] K.M. Abraham, Electrochim. Acta 38 (1993) 1233.
[5] S.S. Zhang, K. Xu, T.R. Jow, J. Power Sources 160 (2006) 1349.
[6] D.D. MacNeil, J.R. Dahn, J. Electrochem. Soc. 148 (2001) A1211.
[7] H. Arai, M. Tsuda, K. Saito, M. Hayashi, Y. Sakurai, J. Electrochem. Soc. 149 (2002) A401.
[8] B.E. Conway, Electrochemical Supercapacitor-scientific Fundamentals and Technological Application, Kluwer Academic, New York, 1999, pp. 29–31.
[9] A. Burke, J. Power Sources 91 (2000) 37.
[10] O. Barbieri, M. Hahn, A. Herzog, R. Kotz, Carbon 43 (2005) 1303.
[11] M. Hahn, A. Warsig, R. Gallay, P. Novak, R. Kotz, Electrochem. Commun. 7 (2005) 925.
[12] G.G. Amatucci, F. Badway, A. Dupsquier, T. Zheng, J. Electrochem. Soc. 148 (2001) A930.
[13] H. Li, L. Cheng, Y. Xia, Electrochem. Solid-State Lett. 8 (2005) A433.
[14] M. Yoshio, H. Nakamura, H. Wang, Electrochem. Solid-State Lett. 9 (2006) A561.
[15] H. Wang, M. Yoshio, Electrochem. Commun. 8 (2006) 1481.
[16] H. Wang, M. Yoshio, A.K. Thapa, H. Nakamura, J. Power Sources 169 (2007) 365.
[17] A.K. Thapa, G. Park, H. Nakamura, T. Ishihara, N. Moriyama, T. Kawamura, H. Wang, M. Yoshio, Electrochim. Acta 55 (2010) 7305.
[18] N. Gunawardhana, G. Park, N. Dimov, A.K. Thapa, H. Nakamura, H. Wang, T. Ishihara, M. Yoshio, J. Power Sources 196 (2011) 7886.
[19] N. Gunawardhana, G. Park, A.K. Thapa, N. Dimov, M. Sasidharan, H. Nakamura, M. Yoshio, J. Power Sources 203 (2012) 257.
[20] N. Kumakai, K. Tanno, Denki Kagaku 50 (1982) 704.
[21] N. Koshiba, K. Takata, M. Nakanishi, Z. Takehara, Denki Kagaku 62 (1994) 593.
[22] N. Koshiba, K. Takata, M. Nakanishi, Z. Takehara, Denki Kagaku 62 (1994) 631.
[23] R.E. Franklin, Acta Crystallogr. 4 (1951) 235.
[24] D. Aurbach, H. Teller, M. Koltypin, E. Levi, J. Power Sources 119–121 (2003) 1.
[25] M. Holzapfel, H. Buqa, F. Krumeich, P. Novak, F.M. Petrat, C. Veit, Electrochem. Solid-State Lett. 8 (2005) A516.
[26] R.T. Carlin, H.C. De Long, J. Fuller, P.C. Frulove, J. Electrochem. Soc. 141 (1994) L73.
[27] P.W. Ruch, M. Hahn, F. Rosciano, M. Holzapfel, H. Kaiser, W. Scheifele, B. Schmitt, P. Novak, R. Kotz, A. Wokaun, Electrochim. Acta 53 (2007) 1074.
[28] Z. Zhang, M.M. Lerner, J. Electrochem. Soc. 140 (1993) 742.
[29] J.A. Seel, J.R. Dahn, J. Electrochem. Soc. 147 (2000) 892.
[30] H. Wang, M. Yoshio, J. Power Sources 177 (2008) 681.
[31] J.P. Olivier, M. Winter, J. Power Sources 97–98 (2001) 151.
[32] F. Cao, I.V. Barsukov, H.J. Bang, P. Zaleski, J. Prakash, J. Electrochem. Soc. 147 (2000) 3579.